Journal of Hydroscience and Hudraulic Engineering
Vol. 4, No. 2, November, 1986, pp.55-69.

INFLUENCE OF WATER SURFACE ON SCOUR FROM VERTICAL SUBMERGED JET

By

N. Akashi

Associate Professor, Department of Civil Engineering
Nishinippon Institute of Technology,
Kanda, Miyako-gun, Fukuoka 800-03, Japan

and

T. Saitou

Professor, Department of Civil Engineering
Yamaguchi University, Ube, Yamaguchi 755, Japan

SYNOPSIS

In the case of scour from a vertically submerged plane jet under shallow tailwater, there exists a threshold flow period during which the shape of the ridge formed downstream from the scour hole is deformed from a triangular shape to a trapezoidal shape, and after which the volume of the scour increases more than under deep tailwater. Scour volume is determined by the transport rate of the suspended sediment through the crest of the triangular ridge or through the upstream edge of the trapezoidal ridge. The formation of a scour hole depends solely on a balance between a force due to a change in momentum flux and the pressure of the submerged sand, regardless of whether the tailwater is deep or not. Threshold values for the tailwater depth and the threshold flow period influencing the scouring process are made clear.

INTRODUCTION

Scours from vertical submerged jets have been regarded as a simplified model for studying scours from plunging jets into deep tailwater from hydraulic outlets, weirs and spillways. Rouse(9) studied erosion due to a plane-half jet: Akashi and Saitou ((1) and (2)) a plane jet; and Doddiah et al.(5), Poreh and Hefez (7), Westrich and Kobus(11), Rajaratnam and Beltaos(8), and Mih and Kabir(6) circular jets. The characteristic lengths of the eroded bed profile have been dealt with in terms of an impingement height(i.e., the distance from the nozzle to the original bed level) equivalent to the plunging water depth. Most practical cases of plunging jets occur under shallow tailwater conditions. In such cases, the influence of the free water surface on the scouring process is clear, as shown in Fig.1: the deflected jet along the inner flank in the scour hole does not diffuse upward but rapidly changes its direction horizontally because of restriction by the water surface; and the ridge is deformed from a triangular to a trapezoidal shape. But there are very few reports considering the influence of the water depth on scours from a vertical submerged jet with a short impingement height.

This paper presents an interpretation of scouring process under shallow tailwater related to the scour mechanisms characterized for the case of a scour under deep tailwater by the authors(2), together with test results for the characteristics of the scour profile and the threshold conditions for the tailwater depth influencing the eroded bed profile.

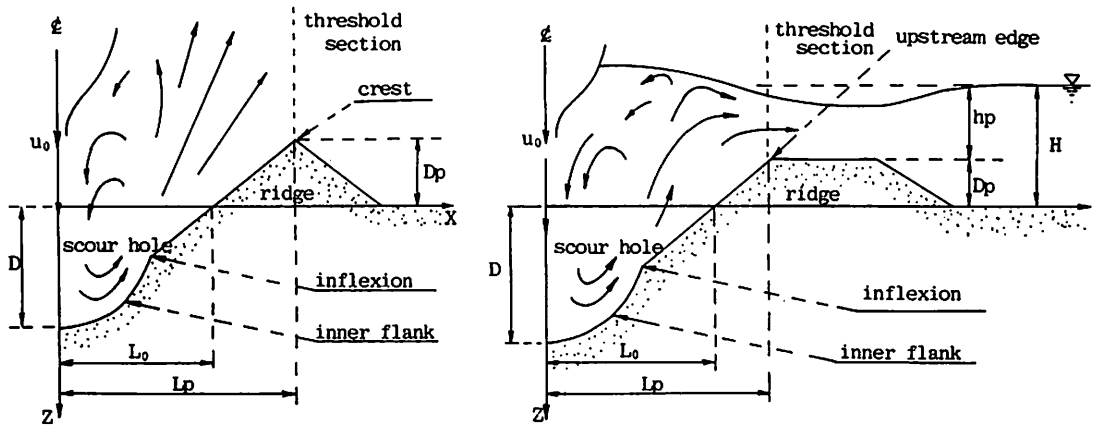

Fig. 1 Definition sketch of scour profile:
a); scour under deep tailwater b); scour under shallow tailwater

EXPERIMENTAL EQUIPMENT AND PROCEDURE

A schematic diagram for the experimental apparatus is shown in Fig. 2. The basic apparatus is a tank 2 m in length, 0.2 m in width and 1 m in depth, with a vertical jet nozzle fitted from over the tank. The tank is made of a steel frame and acrylic glass walls. The nozzle width B_0 is 2 cm.

Experimental variables are issuing velocity u_0 at the nozzle, impingement height h, tailwater depth H and mean diameter d of a grain of uniform sand. Table 1 shows the range of experiments.

The experiments were carried out as follows. The sand surface and the tailgates of both sides of the test tank were set at a given level respectively; the nozzle chamber was filled with water and the nozzle submerged into the still water. The jet was started by flash-operating a butterfly-valve. The discharge was measured with two containers of 0.5 m^3 set near both sides of the test tank. Time variations of the eroded bed profile were photographed with a motor-drive-camera and a video camera. In the tests, the maximum duration of the flow was 4 hours; when the ridge reached the tailgates in less than 4 hours, then the flow was stopped.

DESCRIPTION OF SCOURING PROCESS

The block diagram in Fig.3 gives a physical interpretation of the scouring process in three stages. The state of movement of the bed and the flow field

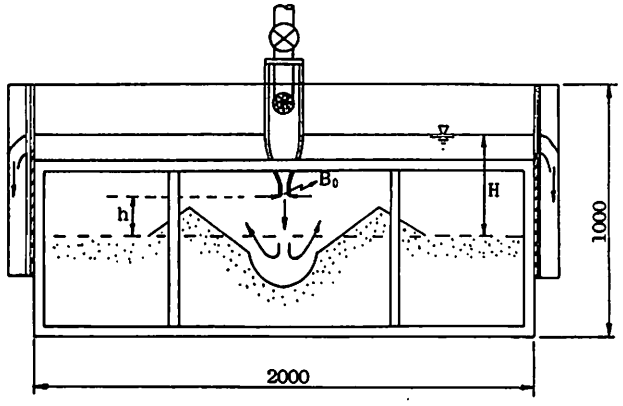

Fig.2 Schematic diagram of experimental apparatus (unit in mm)

Table 1 Experimental conditions

B_0	2 cm
h/B_0	0 ∿ 10
d/B_0	0.035 ∿ 0.121
u_0^2/sgd	12 ∿ 360
H/B_0	3.5 ∿ 30

determining it are shown together with the various shapes of the eroded bed.

In the early stage, the deflected jet flows almost horizontally and the rate of scour is determined by the sediment transport rate as bed load varying spatially.

In the middle stage, the rate of scour is influenced by a separately deflected jet caused by the slope of the inner flank of the scour hole becoming gradually steeper over time.

In the last stage, part of the upstream side of the ridge becomes unstable, with a slope steeper than the angle of repose for the sand particles. This part begins to slide intermittently toward the eroded zone in the center because of unbalance in the forces acting on the inner flank due to the swaying of the jet. The eroded bed takes on a transiently stable profile having an inflexion at the intersection of the inner flank and the upstream slope of the ridge produced by a balance in forces. The sand is carried along the inner flank as bed load, and, beyond the inflexion point, in suspension. Under deep tailwater, the deflected jet is diffused straight, upward and obliquely. The shape of the ridge is triangular. The rate of scour is determined by the rate of the transport in suspension over the crest of the ridge (threshold section). Under shallow tailwater, however, the deflected jet from the scour hole rapidly changes its direction horizontally due to restriction by the water surface. The velocity of the horizontal flow gradually increases as the height of the crest increases(i.e., the depth of the water on the crest decreases), so that the sand particles settled near the crest of the triangular ridge are moved downstream by the tractive force

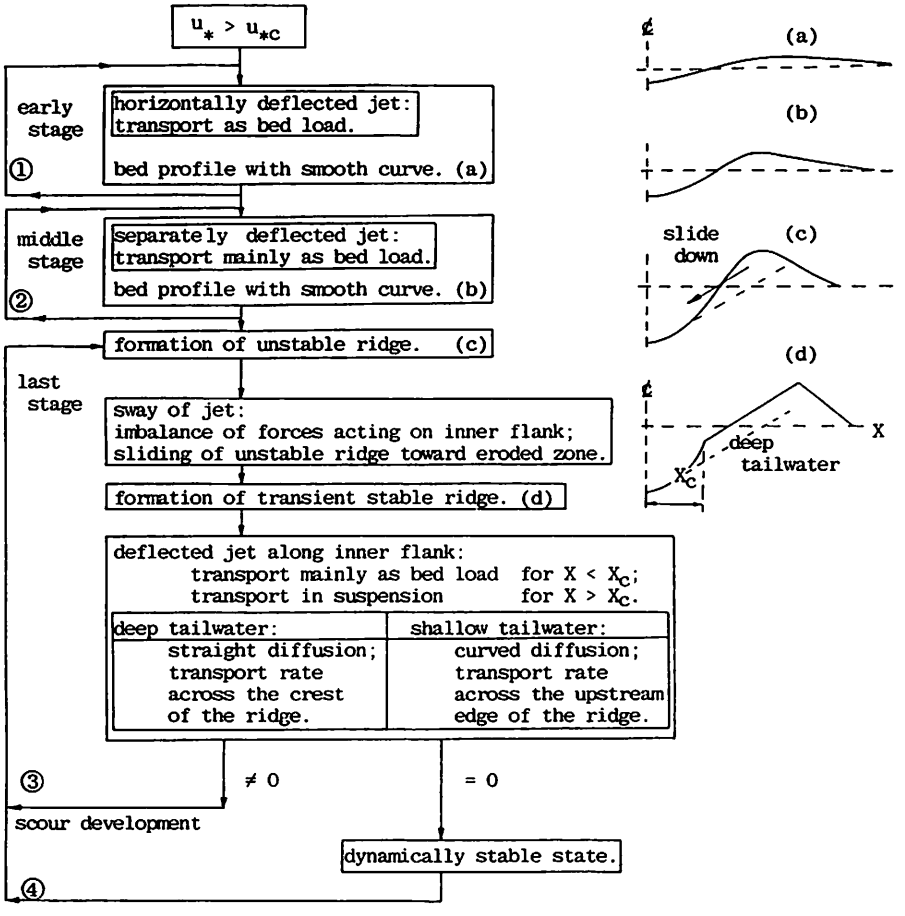

Fig. 3 Block-diagram of scour process

due to the horizontal flow. Eventually, the ridge is deformed from a triangular shape to a trapezoid. The rate of scour is determined by the transport rate at the upstream edge of the ridge (threshold section): almost all of the sand particles settled downstream from the upstream edge of the ridge are carried away by the tractive force. After a very long time, the scouring process appears to reach a dynamically stable state, symbolized by the feedback-line 4, at which the transport rate through the threshold section becomes zero.

EXPERIMENTAL RESULTS

Eroded Bed Profiles

One example of the evolution of an eroded bed profile influenced by the water surface is shown in Fig.4. During the first 4 sec of the observation period the scouring process is in the middle stage; and after 8 sec the last stage. Under the conditions of a jet with high velocity and a short impingement height, it is very difficult to observe the early stage. The water surface apparently has no effect from 15 sec to 240 sec: the ridge keeps a clear triangular shape and the locus of the crest is almost a straight line as pointed out by Rouse(9). After 240 sec, however, when the influence of the water surface on the ridge becomes appreciable, the height of the ridge stops increasing and the crest length of the ridge gradually increases. The water surface profile also varies in time as the crest length increases; the transient flow over the ridge appears to resemble a flow over a submerged broad crest weir.

The four transient eroded bed profiles observed at 2 hours, shown in Fig.5, suggest the existence of a certain threshold tailwater depth. The volume of the scour hole increases when the tailwater depth becomes less than this threshold depth. In the tests the sand particles settled down near the crest appeared to move when the depth of the water over the crest was less than a certain value. This indicates that the influence of the water surface depends not only on the

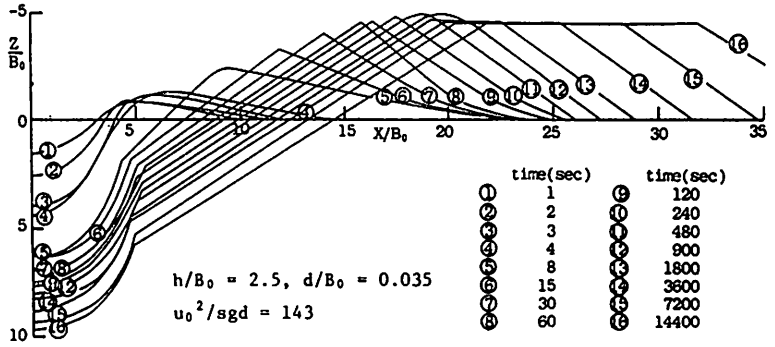

Fig. 4 Evolution of eroded bed profile

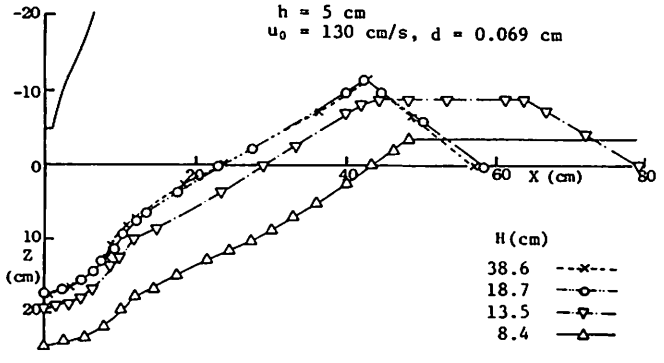

Fig. 5 Eroded bed profile at the time of 2 hours

tailwater depth but also on the height of the triangular ridge. Similarities in the last stage of the eroded bed profile are examined in Figs. 6, 7, 8 and 9 by plotting Z/D against X/L_p, in which D = the maximum scour depth ; and L_p = the distance from the center of the scour hole to the crest of the ridge. Figs. 6 and 8 show the results of the influenced case and the uninfluenced case by the water surface, respectively. Figs. 7 and 9 show the profiles of the scour hole at observation times drawn out from Figs. 6 and 8 respectively. Fig.7 shows that in the uninfluenced case the scour hole profiles do not evolve through similar forms, although at first sight the scour hole profiles shown in Fig.6 seem to be similar. If the scour hole profile kept a similar form, the height of the inner flank would increase with time in proportion to the maximum scour depth: the force of the earth pressure acting on the inner flank would increase with time also. However, since the momentum flux flowing into the scour hole ought not to increase under the increase in the scour depth, the actual height of the inner flank should be considered to lessen or keep a constant value over time. This argument indicates that the similarity of the scour hole profile must be discussed on the basis of a kinematic condition (i.e., the balance between a force caused by the change in flow direction and the pressure of the sand on the inner flank).

Another expression for the eroded bed profile is shown in Fig.10 by plotting Z'/B_0 against X/B_0 where Z' is a vertically upward axis with origin at the maximum scour depth varying over time. Fig.10 shows that under one set of scouring conditions, the profile of the inner flank is uniquely approximated by one curve,

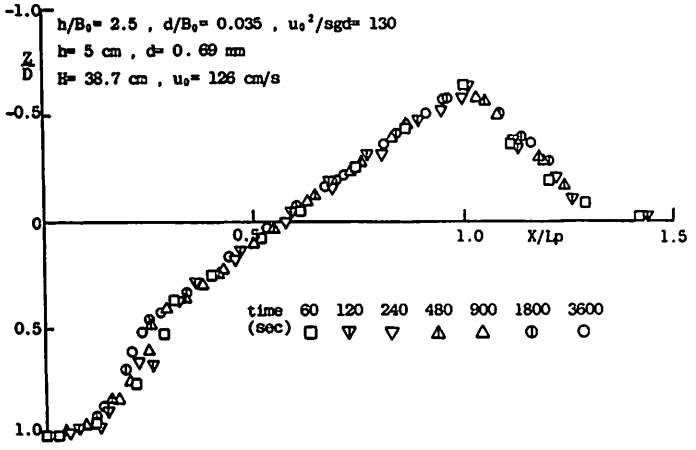

Fig. 6 Similarity of scour profiles in time (under deep tailwater)

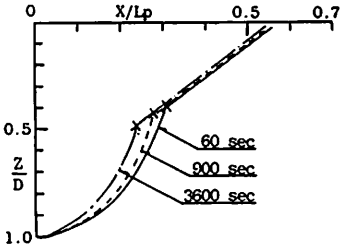

Fig. 7 Profiles of scour hole (under deep tailwater)

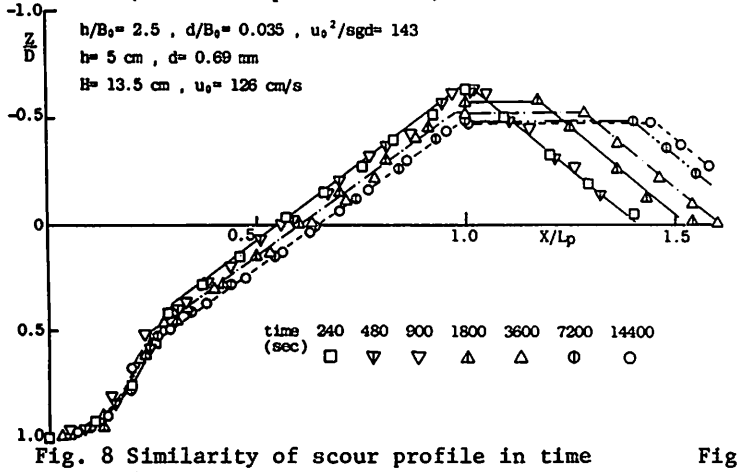

Fig. 8 Similarity of scour profile in time (under shallow tailwater)

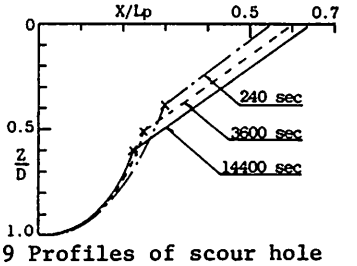

Fig. 9 Profiles of scour hole (under shallow tailwater)

as shown by the solid line, which may be described by the following equation:

$$Z'/B_0 = a \cdot (X/B_0)^2 \qquad (1)$$

Plotting the values of the above coefficient a , which were obtained from many test results, against the impingement height h/B_0 in Fig.11 shows that for impingement heights greater than 3, the curvature of the inner flank decreases against the impingement height, and for impingement heights less than 3, it is almost constant. Assuming that a depends only on the impingement height, although the variable parameters of jet velocity at the nozzle, diameter of sand particles and tailwater depth also appeared to contribute to the form of the inner flank in the test observations, its values can be approximated as:

$$a \fallingdotseq \begin{cases} 0.178 & \text{for } h/B_0 < 3 \\ 0.42 \cdot (h/B_0)^{-0.78} & \text{for } h/B_0 > 3 \end{cases} \qquad (2)$$

The above equations are drawn with a solid line in Fig.11.

In order to investigate the height of the inner flank, a model for the balance of forces acting on the inner flank was proposed (Akashi and Saitou(2)), as shown in Fig.12. F is the force due to the change of momentum flux in the horizontal direction and P is the horizontal force of the sand pressure acting on the inner flank between $X = X_a$, at which the tangential line has the angle of repose, and $X=X_c$, the inflexion point. Assuming the inner flank is a solid wall, the horizontal force P can be obtained by applying Coulomb's Formula for active earth pressure as follows:

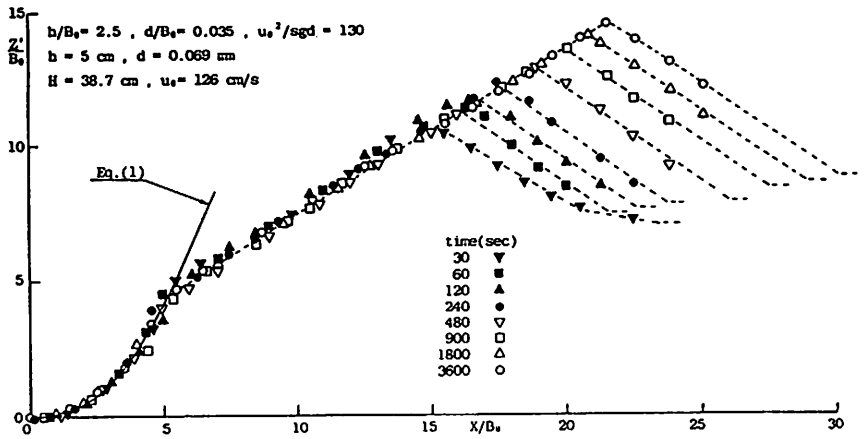

Fig.10 Similarity of scour hole profile

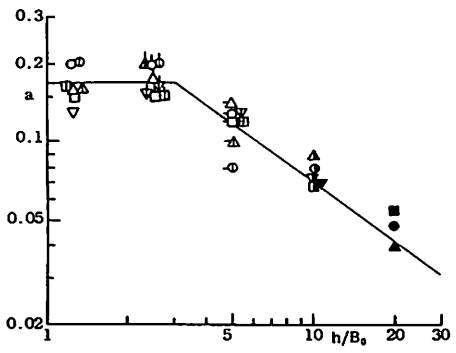

h/Bo	d/Bo	uo cm/s	H cm	key	shape of ridge
1.25	0.056	116	11	○	△
		128	11	△	△
		185	11	□	△
		190	16	▽	△
	0.121	115	11	⊕	△
		155	11	⊿	△
		192	11	▥	△
2.5	0.056	117	11	◇	△
		145	11	△	△
		190	11	⊡	△
		190	21	▽	△
	0.121	117	11	◈	△
		152	11	⊿	△
		190	11	⊞	△
		190	21	▽	△

h/Bo	d/Bo	uo cm/s	H cm	key	shape of ridge
5	0.069	90	18	⊿	△
		131	19	○	△
		131	13.5	□	△
	0.021	30	30	⊕	△
		123	30	⊿	△
	0.042	74	30	▥	△
		150	30	▽	△
10	0.069	74	24	●	△
		130	24	▲	△
	0.021	32	40	■	△
	0.042	121	40	▽	△
		149	40	▼	△
20	0.021	60	60	●	△
		118	60	▲	△
	0.042	160	60	■	△

Fig.11 Coefficient of parabolic curve for scour hole profile

$$P = 1/2 \cdot f(\theta) \cdot s g H_z^2$$

$$f(\theta) = \frac{\sin^2(\theta-\phi)}{\sin^2\theta \cdot \sin(\theta+\phi')} \left\{ 1 + \sqrt{\frac{\sin(\phi+\phi') \cdot \sin(\phi-i)}{\sin(\theta+\phi') \cdot \sin(\theta-i)}} \right\}^{-2} \qquad (3)$$

where H_z = the difference between the heights at $X=X_c$ and $X=X_a$; s= the specific gravity of submerged sand particles; g= the acceleration due to gravity; θ = the angle between the tangential line at $X=X_c$ and the horizontal line; i= a grade of the upstream slope of the ridge taking the same value as the angle of repose for the sand particles; ϕ'= zero as the friction angle between the assumed solid wall and the sand particles; and ϕ= the internal friction angle of the sand particles taking the same value as the angle of repose of uniform sand particles. Assuming that the momentum fluxes in the horizontal direction through the sections at $X=X_a$ and $X=X_c$ are M and $M \cdot \cos\theta$ respectively, and that the velocity profile in the section at $X=X_a$ is similar to a half plane free jet, F can be obtained as follows:

$$F = M \cdot (1 - \cos \theta) \qquad (4)$$

$$M = 2\rho u_m^2 \delta_0 \; / \; (3 \cosh^{-1} \sqrt{2}) \qquad (5)$$

where u_m = the maximum velocity in the section; and δ_0 = the representative length scale at which the velocity is equal to half of the maximum velocity. Furthermore, assuming that a horizontal solid bed lies at the level of the maximum scour depth, the following equations, which have been given before (2), can be applied for the values of u_m and δ_0 at $X=X_a$:

$$\frac{\delta_0}{B_0} = 0.124 \cdot \left\{ \frac{X}{B_0} + \frac{1}{3} \cdot \frac{h}{B_0} + 2.30 \right\} \qquad (6)$$

$$\frac{u_m}{u_0} = \frac{u_j}{u_0} \cdot \frac{u_m}{u_j} \qquad (7)$$

$$\frac{u_j}{u_0} = \sqrt{7.2 \; / \; (\frac{h}{B_0} + 3.2)} \qquad (8)$$

$$\frac{u_m}{u_j} = \begin{cases} 4 \, \alpha_h \, X/h & \text{for } \alpha_h X/h < 0.25 \\ 1 & \text{for } 0.25 < \alpha_h X/h < 0.5 \\ \sqrt{0.9 \; / \; (\alpha_h \, X/h + 0.4)} & \text{for } 0.5 < \alpha_h X/h \end{cases} \qquad (9)$$

$$\alpha_h = - (0.00655 + 0.0315 \frac{d}{B_0}) \cdot (\frac{h}{B_0})^2 + (0.188 - 0.71 \cdot \frac{d}{B_0}) \cdot (\frac{h}{B_0}) + 0.262 - 2.05 \cdot \frac{d}{B_0} \qquad (10)$$

where $\alpha_h \geq 1$; u_j= the maximum velocity at the final edge of the stagnant region.

From the above model and the profile of the inner flank in Eq.(1), the height and the width of the inner flank can be computed by using a trial-and error method as shown by the flow chart in Fig.13: X_a is determined from h/B_0 using Eqs.(1) and (2); F and P are calculated from u_0, B_0, D, h and d using Eqs.(3) to (10) by taking the movement of an assumed point along the curve of Eq.(1); the inflexion point($X = X_c$, at which F = P) is determined.

Fig.14 shows that for the observed profile of the inner flank just before the flow was stopped the calculated values for X_c agree well with the experimental results. This indicates that the formation of the inner flank can be adequately explained by this kinematic model.

Characteristic Lengths of the Eroded Bed Profile

Figs.15, 16 and 17 show experimental results for the height D_p/B_0 of the

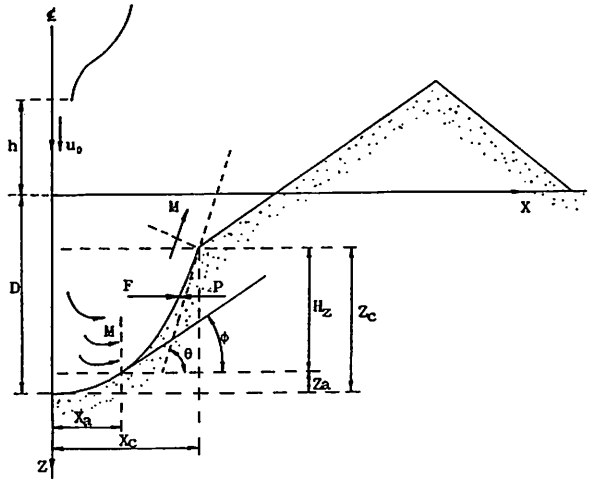

Fig.12 A model for the balance of forces acting on the inner flank

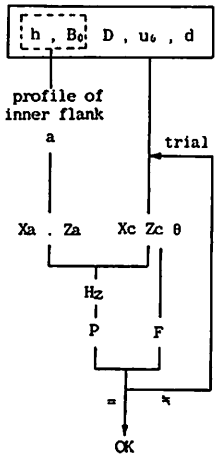

Fig.13 Procedure of calculation for the inner flank

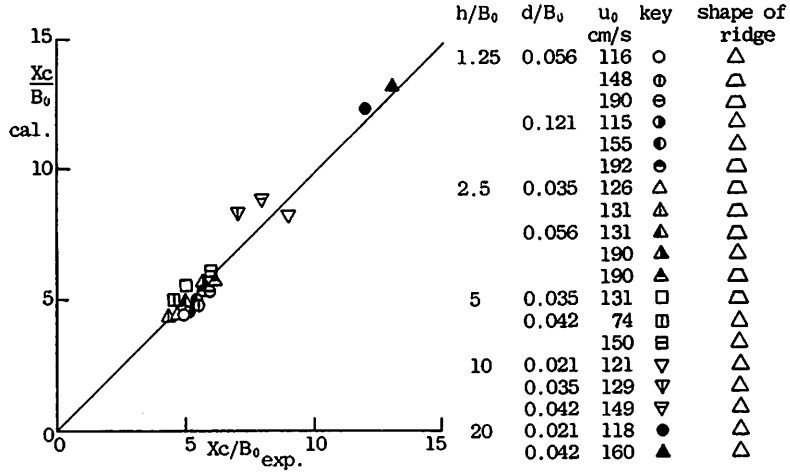

Fig.14 Comparison of the experimental results with the calculated results

ridge, the distance L_p/B_0 of the threshold section from the center of the scour hole and the length L_0/B_0 of the scour hole, plotted against the maximum scour depth D/B_0. In these figures, the arrows indicate the starting points for the last stage of the scouring process; the solid lines and the dotted lines are the mean lines for the uninfluenced and the influenced cases, respectively.

Fig.15 shows that for the uninfluenced case, log D_p/B_0 increases linearly with log D/B_0 in the last stage, but that for the influenced case the variation of log D_p/B_0 deviates from this trend: the value of D_p/B_0 becomes gradually smaller against the development of D/B_0, and appears to reach an asymptotic value. At the same jet velocity, the value of D/B_0 for the influenced case was larger than that for the uninfluenced case, as one would expect.

Fig.16 shows that logL_p/B_0 is linear to logD/B_0 in the last stage of both the uninfluenced case and the influenced case, with the curve for the former having a steeper slope than that for the latter.

Fig.17 also shows that log L_0/B_0 is linear to log D/B_0 in the last stage. Another interesting observation is that the data points in the last stage for the influenced case lie above the respective line extrapolated from those for the

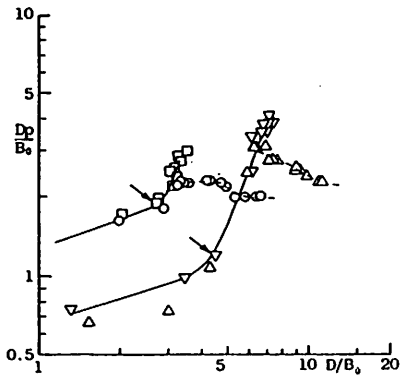

Fig.15 Relation between D_p/B_0 and D/B_0

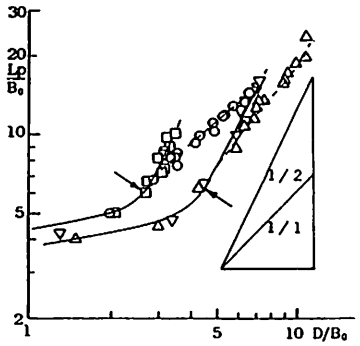

Fig.16 Relation between L_p/B_0 and D/B_0

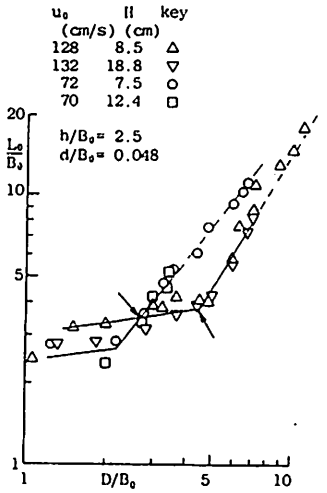

Fig.17 Relation between L_0/B_0 and D/B_0

uninfluenced case. This indicates that the scour hole is formed by a similar mechanism regardless of whether the ridge is influenced by the water surface or not.

Before discussing the experimental results for the maximum scour depth, the development of the maximum scour depth in the last stage is considered on the basis of the continuity of sediment transport.

Letting the actual scour volume in a time interval of Δt take a value q_p equal to the rate of sediment transport in suspension across the crest or the upstream edge of the ridge, and assuming that during this interval the eroded depth ΔZ in the zone from the center to the threshold section is almost same (as shown in Fig.4), the rate of change of the eroded depth is:

$$\frac{\Delta Z}{\Delta t} \propto \frac{\Delta Z_0}{\Delta t} \propto q_c \cdot \frac{q_p}{q_c} / L_p \qquad (11)$$

where $\Delta Z_0 = \Delta D$; and q_c= a diffused volume from the scour hole by the upward deflected jet in a time interval of Δt. Rewriting the above equation as a dimensionless form,

$$\frac{\Delta \zeta_0}{\Delta \tau} \propto \Phi_c \cdot \frac{\Phi_p}{\Phi_c} / \xi_p \qquad (12)$$

where $\Phi_p = q_p/\sqrt{sgd^3}$, $\Phi_c = q_c/\sqrt{sgd^3}$, $\xi_p = L_p/B_0$, $\zeta_0 = D/B_0$, and $\tau = u_0^2/sgd \cdot u_0 t/B_0$. Since ξ_p is almost proportional to $\zeta_0^{n_1}$ in the last stage (from the experimental results, the value of the power n_1 is about between 1.0 and 2.0) and Φ_c is nearly equal to the rate of sediment transport in the equilibrium state,

$$\xi_p \propto \zeta_0^{n_1} \qquad (13)$$

and

$$\Phi_c \propto \left\{ \frac{u_0^2}{sgd} \cdot \left(\frac{u*}{u_c}\right)^2 \cdot \left(\frac{u_c}{u}\right)^2 \right\}^{1.5} \qquad (14)$$

where u_c is the maximum velocity in the section at which the sediment transport rapidly changes from transport as bed load to transport in suspension. Based on Eqs.(7) to (9) , u_c is deduced as follows;

$$\frac{u_c}{u_0} \propto (h_0 + \zeta_0)^{-1/2} \qquad (15)$$

where $h_0 = h/B_0$. When the change of ζ_0 is small, u_*/u_c is almost constant in the vicinity of the stagnant point at the center of the scour hole. Accordingly Φ_c can be rewritten as

$$\Phi_c \propto (h_0 + \zeta_0)^{-1.5} \qquad (16)$$

Since the rate of sediment transport in suspension Φ_p/Φ_c is inversely proportional to an exponential function with respect to a distance in the suspension zone (Dobbins(4)),

$$\Phi_p / \Phi_c \propto \exp(- \xi_p) \propto \exp(- \zeta_0^{n_1}) \qquad (17)$$

Combining the above relations, Eq.(12) is reduced to

$$\frac{\Delta\zeta_0}{\Delta\tau} \propto (h_0 + \zeta_0)^{-1.5} \cdot \exp(- \zeta_0^{n_1}) / \zeta_0^{n_1} \qquad (18)$$

Fig.18 shows the relation between the right hand of the above equation and ζ_0 with the parameters h_0 and n_1. Considering that the change in ζ_0 is small in the last stage, it is seen that the right hand in Eq.(18) can be approximately given as the solid lines in Fig.18. Consequently, Eq.(18) is rewritten as follows:

$$\Delta\zeta_0 / \Delta\tau \propto \zeta_0^{n_2} \qquad (19)$$

or,

$$\zeta_0 = m_0 \cdot \tau^{n_0} \qquad (20)$$

where the coefficient m_0 and the power n_0 (or n_2) are determined by the dimensionless parameters of the impingement height h/B_0, the roughness of the bed d/B_0 and the (densemetric) Froude number $(u_0^2/sgd)^{1/2}$. Eq.(20) shows that log ζ_0 is linear to logτ , disagreeing with the results of Rouse(9) which show a semilogarithmic linear relationship.

The evolutions of the maximum scour depth are shown in Fig.19, in which the downward arrows indicate the starting time of the last stage; the upward arrows indicate the time at which the effect of the water surface appeared on the ridge. In the last stage of the uninfluenced cases log D/B_0 increased linearly with logτ, as shown by the respective solid lines, and $d(\log D/B_0)/d(\log \tau)$ (for constant h/B_0 and d/B_0), was independent of the jet velocity. The results before the influence of the water surface appeared are almost the same as the results in the uninfluenced cases, as shown by the dotted lines. On the other hand, the results

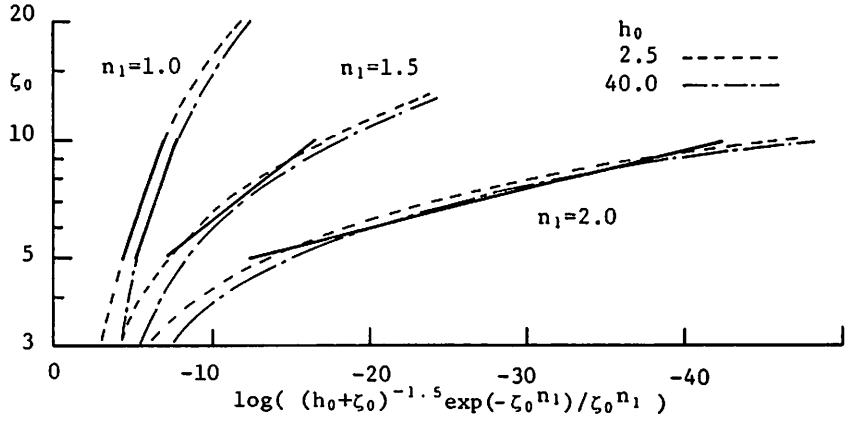

Fig.18 Relation between the right hand in Eq.(18) and ζ_0

after the influence of the water surface appeared shows a different trend with a larger inclination than that in the uninfluenced cases. This change in the inclination can be explained by the following reasons: the development of the ridge height leads to a decrease of the water depth over the crest, in other words an increase in the mean velocity in the threshold section at the crest. Also the distance from the center of the scour hole to the threshold section is relatively shorter for the influenced cases than for the uninfluenced as seen from Fig.16. The rate of sediment transport in suspension through the threshold section becomes large when the presence of the water surface influences the scouring process.

Threshold Values Influencing the Scouring Process

The threshold water depth h_p over the crest of the ridge at the threshold time (after which the effect of the water surface begins to appear on the ridge) is plotted against the jet velocity in Fig.20-a: h_p was estimated as $H - D_p$, since a precise measurement of the water depth could not be made because of the violent fluctuations of the water surface due to the swaying, and the deflexions from the scour hole of the jet. The solid lines in Fig.20-a are drawn as upper limits for the threshold water depth for the respective mean diameter d of sand particles, as the data points are fairly dispersed. Fig.20-b is a rearrangement of Fig.20-a, with h_p/B_0 plotted against u_0/u_{*c} ; the critical friction velocity u_{*c} is assumed to be $u_{*c}^2/sgd = 0.05$. The solid lines in Fig.20-a are consolidated into one line in Fig.20-b, described by the equation:

$$h_p/B_0 = 1/20 \cdot u_0/u_{*c} \qquad (21)$$

As $\overline{u} = u_0 B_0/(2h_p)$, where $\overline{u}$ is the mean velocity in the threshold section, the

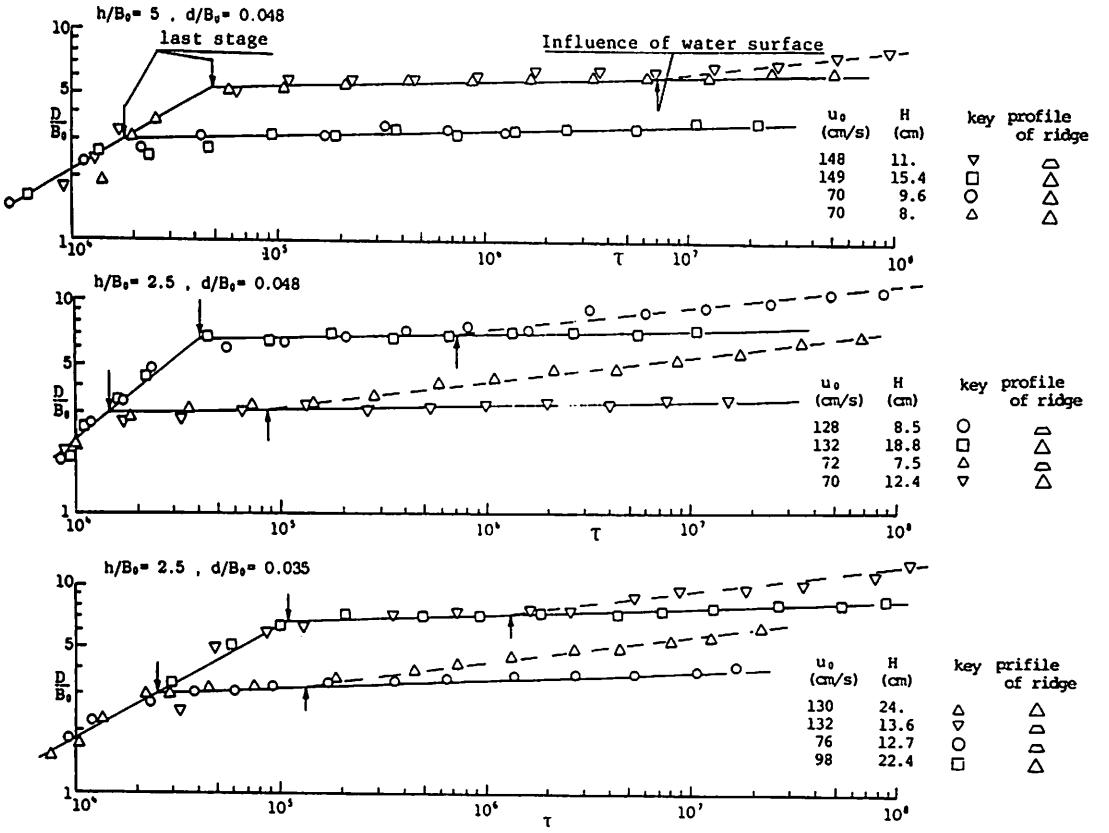

Fig.19 Evolution of maximum scour depth:
comparison of uninfluenced cases with influenced cases

sand particles on the crest of the ridge are carried away when $\overline{u}/u_{*c} > 10$. Consequently, for the threshold tailwater depth H_1, the following equation is given:

$$H_1/B_0 = h_{p1}/B_0 + D_{p1}/B_0 \qquad (22)$$

where D_{p1} is the height of the ridge for a dynamically stable state of the uninfluenced case by the water surface.

When the tailwater depth H is smaller than H_1, the effect of the water surface on the scouring process is determined by the threshold time of the flow period. The threshold times for the respective scour conditions are shown in Fig.21. The solid lines are a crude approximation drawn with the parameter H/B_0, which can be reduced as an experimental equation as follows:

$$\tau_c = 10^5 \cdot \left(1.2 \cdot (H/B_0)^3/(u_0^2/sgd) \right)^m$$

$$m = 0.02 \cdot \left(H/B_0 \right)^3 \qquad (23)$$

From the above considerations, threshold conditions between shallow and deep tailwater and between influenced and uninfluenced scours can be defined as follows:

$H/B_0 > H_1/B_0$ ----- deep tailwater (= uninfluenced case)

$H/B_0 < H_1/B_0$ ----- shallow tailwater

$\tau > \tau_c$ ----- influenced case

$\tau < \tau_c$ ----- uninfluenced case (24)

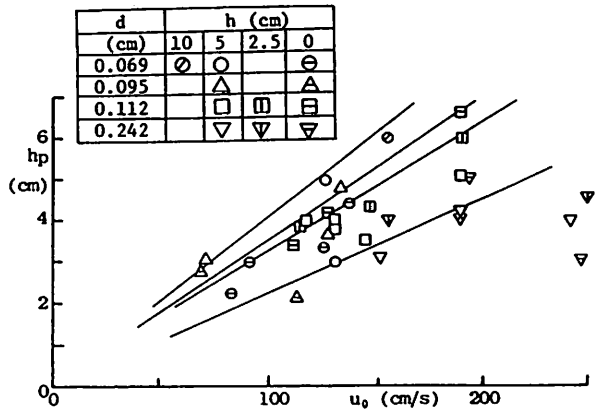

Fig. 20-a Relation between threshold water depth and jet velocity

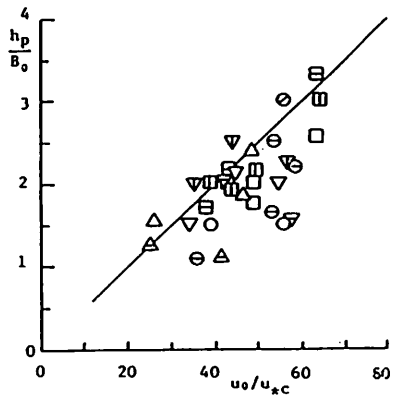

Fig.20-b Relation between h_p/B_0 and u_0/u_{*c}

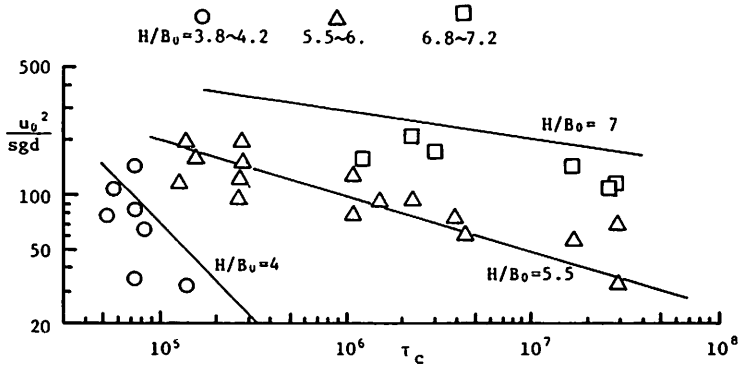

Fig.21 Threshold time at which the shape of the ridge is deformed

CONCLUSIONS

The results obtained in this paper are summarized below:

1) Even in the case of scours under shallow tailwater, it was comfirmed that before a threshold time (after which the effect of the water surface begins to appear on the ridge), the eroded bed profile does not differ from that under deep tailwater.

2) The profiles of the inner flank in the last scour stage(during which the scouring action asymptotically approaches a dynamically stable state), evolve with almost the same form under constant scouring conditions, regardless of whether the tailwater is deep or not. The width and the height of the inner flank can be explained with a kinematic model based on a balance between a force due to changes in the flow direction of the deflected jet and the pressure of the submerged sand.

3) From considerations of the sediment transport in suspension, it was concluded that the maximum scour depth changes with the time in a logarithmic linear relationship, although previous studies have shown this relationship to be semilogarithmic linear. And it was observed that the rate of change of the maximum scour depth for the influenced scour by the water surface becomes larger than that for the uninfluenced scours.

4) A distinction between shallow and deep tailwater was made with experimental equations for the threshold tailwater depth. Furthermore, for shallow tailwater, the threshold time of flow before which the scouring process is little influenced by the water surface was made clear.

ACKNOWLEDGEMENT

This work was partially supported by the Grant-in Aid for Scientific Research(No.57750453) from the Ministry of Education, Science and Culture of Japan.

REFERENCES

1. Akashi, N. and T. Saitou: Estimation of equilibrium scour depth from submerged impinged jet, Proc. 4th Congress of APD-IAHR, pp.167-181, 1984.
2. Akashi, N. and T. Saitou : Studies on the scour from submerged impinged jet Proc. of Japan Society of Civil Engineers, No.298, pp.53-62, 1980.
3. Albertson, M.L., Y.B. Dai, R.A. Jensen and H. Rouse : Diffusion of submerged jets, Transactions of ASCE, Vol.155, pp.639-664, 1950.
4. Dobbins, E.M. : Effect of turbulence on sedimentation, Transactions of ASCE, pp.235-262, 1943.
5. Doddiah, D., M.L. Albertson and R. Thomas : Scour from jets, Proceedings, 5th Congress of IAHR,pp.161-169, 1953.
6. Mih, C.W. and J. Kabir : Impingement of water jets on nonuniform streambed, Journal of Hydraulic Engineering, ASCE, Vol.109, No.4, pp.536-548, 1983.
7. Poreh, M. and E. Hefez : Initial scour and sediment motion due to an impinging jet, Proceedings, 12th Congress of IAHR, Vol.3, pp.9-16, 1967.
8. Rajaratnam, N. and S. Beltaos : Erosion by impinging circular turbulent jets, Journal of the Hydraulics Division, Proc. ASCE, Vol.103, No.HY10, pp.1191-1205, 1977.
9. Rouse, H. : Criteria for similarity in the transportation of sediment, Bulletin 20, Univ. of Iowa, pp.33-49, 1939.
10. Saitou, T., N. Akashi and Y. Kameda : Wall jets owing to plane jet of impinging and reattachment, Memoires of the Faculty of Eng., Yamaguchi Univ., Vol.28-1, pp.31-42, 1977.
11. Westrich, B. and H. Kobus : Erosion of a uniform sand bed by continuous and pulsating jets, Proceedings, 15th Congress of IAHR, Vol.1, pp.91-98, 1973.

APPENDIX - NOTATION

The following symbols are used in this paper:

- a = coefficient denoting the profile of inner flank;
- B_0 = nozzle width;
- d = mean diameter of a grain of uniform sand;
- D = maximum scour depth in the center of the scour hole;
- D_p = height of the ridge;
- D_{pl} = height of the ridge in a dynamically stable state;
- F = a force acting on the inner flank due to the change of momentum flux;
- g = acceleration due to the gravity;
- h = impingement height(distance from nozzle to original bed level);
- h_0 = dimensionless value of $h_0 = h/B_0$;
- h_p = water depth in the threshold section, $h_p = H - D_p$;
- h_{pl} = threshold value of h_p influencing the scouring process;
- H = tailwater depth;
- H_l = threshold value of H influencing the scouring process;
- H_z = height between a point at which a tangential line has the angle of repose and an inflexion point = $Z_c - Z_a$;
- i = angle between a upstream slope of ridge and the horizontal line;
- L_0 = length of scour hole;
- L_p = distance from the center to the crest of the triangular ridge or the trapezoidal ridge;
- m = a power in Eq.(23);
- m_0 = a coefficient in Eq.(20);
- M = momenyum flux;
- n_0 = a power in Eq.(20);
- n_1 = a power in Eq.(13) = $d(\log \xi_p)/ d(\log \zeta_0)$;
- n_2 = a power in Eq.(19);
- P = force due to sand pressure acting on the inner flank;
- q_c = virtual scour volume;
- q_p = actual scour volume in a time interval Δt which is equal to sediment transport in suspension through the threshold section;
- s = submerged specific gravity of sand particles;
- t = scouring time;
- Δt = time interval of scouring time;
- u_c = maximum velocity in the section at which the form of sediment transport changes from transport as bed load to transport in suspension;
- u_j = maximum velocity at the final edge in the stagnant region;
- u_m = meximum velocity in a section;

u_0 = jet velocity issuing at the nozzle;

$\bar{u}$ = mean velocity in the threshold section;

u_* = friction velocity;

u_{*c} = critical friction velocity;

X = horizontal axis with an origin at the original bed level in the center;

X_a = value of X at which the tangential angle of the inner flank has the angle of repose ;

X_c = value of X at which an upper limit of inner flank is given;

Z = eroded depth;

Z_a = value of Z at which $X = X_a$;

Z_c = value of Z at which $X = X_c$;

Z' = a vertical upward axis with an origin at the maximum scour depth;

ΔZ = eroded depth in time interval Δt;

ΔZ_0 = eroded depth in the center in time interval Δt;

δ_0 = representative length where velocity is equal to half of the maximum velocity;

ζ = dimensionless value of Z, $= Z/B_0$;

ζ_0 = value of ζ in the center;

$\Delta\zeta_0$ = dimensionless eroded depth in the center in a time interval Δt;

θ = angle between tangential line at $X = X_c$ and horizontal line;

ξ = dimensionless value of X, $= X/B_0$;

ξ_p = value of ξ in the threshold section;

ρ = mass density of fluid;

τ = dimensionless scouring time $= u_0^2/sgd \cdot u_0 t/B_0$;

τ_c = value of τ at which influence of water surface appears in the ridge;

$\Delta\tau$ = dimensionless scouring time interval;

ϕ = internal friction angle of sand particles;

ϕ' = friction angle between solid wall and sand particles;

Φ_c = dimensionless value of $q_c = q_c/\sqrt{sgd^3}$; and

Φ_p = dimensionless value of $q_p = q_p/\sqrt{sgd^3}$.